Relative Effects on Atmospheric Ozone of Latitude and Altitude of Supersonic Flight

Derek M. Cunnold,* Fred N. Alyea,* and Ronald G. Prinn†
Massachusetts Institute of Technology, Cambridge, Mass.

Three calculations are reported of the potential depletion of ozone by supersonic aircraft. These calculations utilized a two-dimensional model and a three-dimensional photochemical-dynamical model of the atmosphere in which ozone and the dynamical variables of the atmosphere were derived simultaneously. All calculations were based on a continuous atmospheric injection of 1.8×10^6 tons/yr of NO_2. Injections at 45°N and 20 km, at equilibrium, resulted in a 36% increase in total odd nitrogen (NO_y) between 8 and 38 km and in global ozone depletion of approximately 12%. Injection at 45°N and 17 km produced a 27% increase in NO_y, but, because much of this increase occurred below 20 km, the ozone depletion amounted to only 6%. Injection at 10°N and 29 km resulted in a 55% increase of NO_y; however, although there was more depletion above 20 km altitude, there was less below that altitude, and the ozone depletion was only 12.5%. Relative global depletions are judged to be more meaningful than absolute depletions in these calculations. In all three calculations, at least half as much ozone depletion occurred in the Southern Hemisphere as in the Northern Hemisphere.

Introduction

THE environmental impact resulting from the operation of supersonic aircraft such as the Concorde and the Tupolev 144 has been debated vigorously over the past five years; scientific assessments of the problem after several years of research sponsored by the U.S. and European governments are given in Refs. 1-3. However, because of the time constraints under which those reports were written, it was not possible to address questions such as "what is the effect of the latitude of injection of nitrogen oxides (NO_x) on ozone depletion?" In particular, what is the relationship between the ozone depletion for a tropical injection of NO_2 such as would occur during flights between hemispheres and ozone depletion resulting from the more prevalent East-West airlines routes, during which injection takes place at midlatitudes? This paper addresses this question and also the effect of the altitude of injection on ozone depletion.

The effect of cruise altitude on ozone depletion has been considered by several investigators using one-dimensional models of the atmosphere (in which height is the dependent variable). A comparison of ozone depletion for a 20-km midlatitude source of NO_x obtained by one-, two-, and three-dimensional models is given in Ref. 1. It is not possible to determine the differences between tropical and midlatitude injections of nitrogen oxides with a one-dimensional model.

A calculation of equal importance to the determination of the total global ozone depletion is an assessment of the latitudinal variation of this depletion and, in particular, of the depletion to be expected in the Southern Hemisphere for injections in the Northern Hemisphere. In principle, such calculations can be made using two- and three-dimensional models of the atmosphere, but conclusions depend upon one's ability to adequately simulate atmospheric transport. We have previously reported[4] that a preliminary analysis suggested a factor of 2 greater depletion in the Northern Hemisphere than the Southern Hemisphere for a midlatitude source of NO_x at 20 km alt. Widhopf,[5] for the same source conditions, reported an interhemispheric depletion ratio of approximately 4. However, Widhopf[5] used a two-dimensional model with fixed transport parameters believed to be typical of October (a time of year at which cross equatorial transport is probably at a minimum), whereas Alyea et al.[4] used a combination of seasonally varying two-dimensional models of the atmosphere. In this paper, we examine the variation of this interhemispheric depletion ratio with source location.

It is desirable to treat problems of atmospheric chemistry which involve the transport of long-lived atmospheric constituents, particularly ozone, with a three-dimensional model. The principal advantage of using such a model is that the motions responsible for atmospheric constituent distributions need not be parameterized. Thus the transport of each constituent may be influenced by its chemistry, and changes in the ozone concentration are permitted to feedback into changes in the transport rates of all constituents. Ideally then, the NO_x-ozone problem should be treated with a three-dimensional model. However, the large number of chemical reactions needed to treat this problem fully in such a model were expected to require considerably more computer time than was available to us. We therefore chose to predict in our three-dimensional dynamical-chemical model[6] only the one chemical constituent, ozone, which is coupled directly with the dynamics. We were able to include a much more extensive chemistry in an independent two-dimensional parameterized transport model. That model was used to calculate seasonally variable equilibrium NO_x distributions for various source locations; these distributions then were imposed on the three-dimensional model to yield ozone perturbations. Coupling between these two models was minimal. Repeated iterations between models to obtain consistent two-dimensional and three-dimensional transport rates and ozone and nitrogen oxide distributions might have improved the authenticity of these calculations, but such an approach would have made substantial additional demands on computer time. We report calculations of ozone depletions for three source locations: 45°N, 20 km; 45°N, 17 km; and 10°N, 20 km.

Calculated NO_x Distributions

The NO_x calculations were performed using a two-dimensional model of the atmosphere[8,9] which extended from 8 to 38 km with 1 km vertical resolution. This model included the chemistry of odd oxygen, odd hydrogen, and odd nitrogen (with N_2O_5 omitted). The following chemical species were calculated from chemical equilibrium equations: $O(^3P)$, $O(^1D)$, OH, HO_2, H, H_2O_2, and the ratio of NO to NO_2. Profiles of H_2O, CH_4, and CO were prescribed based on observations (see Ref. 8). Three additional species, NO_y

Received July 9, 1976; revision received Nov. 29, 1976.
Index category: Atmospheric, Space, and Oceanographic Sciences.
*Research Associate, Department of Meteorology.
†Associate Professor, Department of Meteorology.

($=NO+NO_2+HNO_3$), NO_x ($=NO+NO_2$), and N_2O, were predicted from continuity equations. In those equations, the motions were assumed to consist of winds (v and w) and eddy transports that were represented by diffusion coefficients (K_{yy}, $K_{yz}=K_{zy}$, K_{zz}). Integration of the model was accomplished with 3-hr time steps, with winds and diffusion coefficients remaining fixed (at seasonal-mean values) for 90 days. During each 90-day period, the ozone distribution also was assumed to remain fixed at seasonal-mean observed values. Not only did this procedure remove one potential source of error in evaluating NO_x distributions, but it also reduced computation time considerably by allowing photodissociation rates to be precomputed using a seasonal-mean solar declination angle. After 90 days of integration, the winds, diffusion coefficients, ozone, and photodissociation rates (and the temperature distribution) suddenly were changed. Integration thus proceeded over four seasons (360 days) using four different sets of parameters and then continued into the second year by returning to the first set of parameters. This technique permitted the model to be seasonally variable. In this model, the Southern Hemisphere was assumed to be dynamically similar to the Northern Hemisphere with a phase lag of 180 days.

The ozone concentrations used in this model were seasonally and zonally averaged concentrations obtained from Northern Hemisphere data derived by Hering.[10-13] Above 10 mb, where the observations were inadequate, ozone mixing ratios were assumed to be independent of height. There are several sets of transport parameters in use in models of this type based upon observations of both active and inactive tracers in the stratosphere. We used values of v and w and K_{yy}, K_{yz}, and K_{zz} from Gudiksen et al.[14] which had been found to describe the spread of tungsten 185 adequately after the Hardtack test series of 1958. From a consistency viewpoint, it might have made more sense to have used transport coefficients derived from our three-dimensional model. As previously stated, this approach was rejected, however, principally because of computer time considerations. Moreover, it is not clear that ozone (on which transport coefficients would have to be based) is transported in the same way as a species such as NO_y.

The lower boundary condition in this model was based upon the assumption that the mixing ratio of NO_y or $HNO_3(f_i)$ was zero at the ground and that these species were rained out with a time constant of 30 days in the 0–8-km region. We can then show[9] that the boundary condition at 8 km reduces to a destruction rate econdition that

$$f_i(8\,\text{km})/f_i(9\,\text{km})=0.8$$

in which the numerical constant, 0.8, is derived from the average vertical transport rate (e.g., $K_z=2\times10^5$ cm^2/sec) and the rainout time in the 0–8-region. This type of boundary condition allows the mixing ratios of NO_y and HNO_3 at 8 km to vary for different stratospheric injection rates of nitrogen oxides.

The upper boundary condition (at 38 km) on NO_x and NO_y in this model was a zero flux condition. Observations of NO_x summarized by Ackerman[15] suggest that the NO_x mixing ratio increases relatively little above 38 km. Above that level, photodissociation becomes an important loss process for NO_x. A subsequent two-dimensional model calculation performed by extending this model to 68 km has shown that, when the photodissociation of NO is included, the maximum NO_x mixing ratio is at 38 km except in a limited latitudinal area in the vicinity of the polar night.

Using this two-dimensional model, calculations of the distribution of odd nitrogen and odd hydrogen in the unperturbed atmosphere first were performed. These time-dependent calculations were continued until the seasonal distributions repeated annually. The resulting distributions of NO_x and HO_x have been reported by Prinn et al.[9] The total

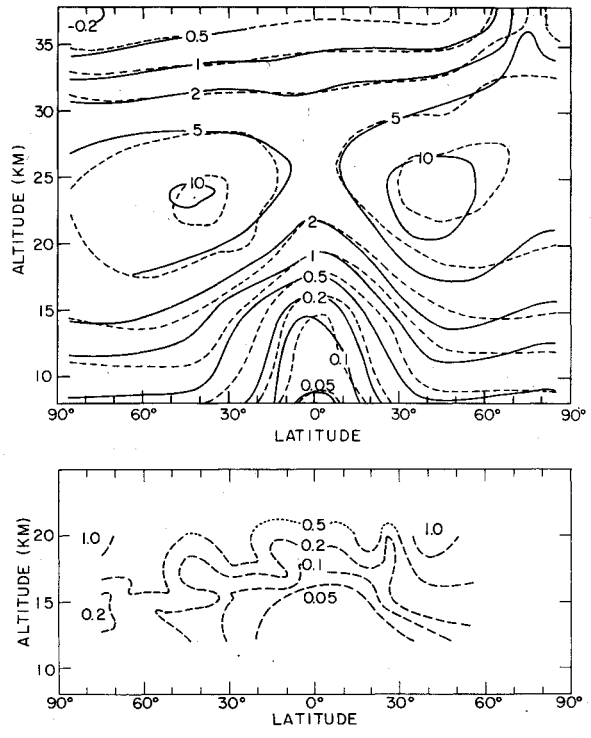

Fig. 1 Computed HNO_3 mixing ratios in the stratosphere. The units are parts per billion by volume. Solid lines represent summer (July–September in the Northern Hemisphere or January–March in the Southern Hemisphere) on the left-hand side and winter on the right-hand side. Dashed lines represent spring (April–June in the Northern Hemisphere or October–December in the Southern Hemisphere) on the left-hand side and fall on the right-hand side. These computed mixing ratios may be compared against the measurements during Northern Hemisphere spring which are presented in the lower part of the illustration (from Lazrus and Gandrud[23]).

odd nitrogen between 8 and 38 km was 1.03×10^{35} molecules. The observations of NO, NO_2, and HNO_3 in the stratosphere unfortunately do not permit any detailed quantitative verification of the predicted distributions. The modeled distribution of HNO_3 has qualitatively the same horizontal and vertical structure as an observed distribution based on a single series of observations in the lower stratosphere, together with several isolated observations at higher altitude (see Fig. 1). The model results for NO_2 in the unperturbed stratosphere are shown in the upper portion of Fig. 2.‡ In these calculations, photodissociation coefficients were averaged over the day in order to eliminate diurnal variations from the model; the species concentrations thus correspond approximately to 24-hr mean values. The comparison of calculated NO_2 and NO concentrations with observations is discussed in Ref. 9, where the calculated concentrations are shown to lie comfortably within the range defined by most of the observations. At high latitudes in winter, NO_2 concentrations are up to an order of magnitude larger than Noxon's observations[16]; this is probably the result of neglecting N_2O_5 in the model chemistry. This disagreement should not have a significant effect on the results of this paper because of the relatively small total area occupied by high latitudes and the small ozone destruction that occurs there in winter.

The chemistry of the two-dimensional model assumed a rate constant for the $OH+HO_2$ reaction of 2×10^{-10}

‡The NO_2 distributions in Prinn et al.[8] differ somewhat from distributions given in Prinn et al.[9] principally because of minor changes in OH chemistry and a different numerical value for the lower boundary condition. Conditions in this paper are similar to those in Ref. 8.

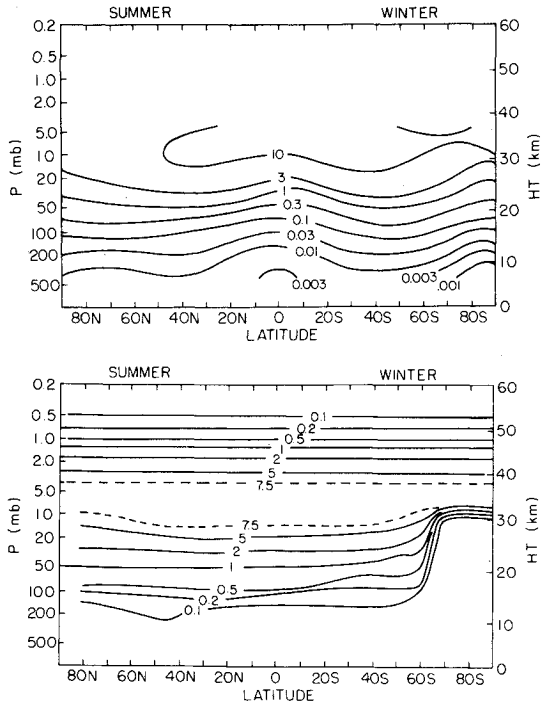

Fig. 2 The two-dimensional calculated NO_2 mixing ratios in the unperturbed stratosphere during the Northern Hemisphere summer are shown in the upper part of the figure. The lower part of the figure shows the result of a two-dimensional calculation by Hesstvedt.[19] Units are parts per billion by volume. Calculated mixing ratios during Northern Hemisphere winter are obtained by reversing the direction of the horizontal axis to yield the South Pole on the left and the North Pole on the right.

cm^3/sec. There is recent evidence that the rate constant for this reaction may be an order of magnitude slower than this. If so, OH concentrations would be approximately three times larger than have been calculated; additional evidence of larger OH concentrations is provided by recent measurements by Anderson.[17] Such a change in rate constants would lead to somewhat smaller NO_x concentrations because of additional conversion of NO_x to HNO_3.

We shall refer to the preceding "steady-state" distributions as existing at time zero. During March of year zero, an additional continuous source of NO_2 at a particular location was added, and the computation was restarted. The first computation was for an NO_2 source of magnitude 1.8×10^6 tons/yr inserted at the 20-km level and distributed in the ratios 1:2:1 at latitudes 50°, 45°, and 40°N. NO_y built up rapidly in the first two years in the source region, but the accumulation was delayed by several years in the Southern Hemisphere as a result of the slow interhemispheric transfer, which, in this model, occurred more slowly than some observations of the atmosphere suggest (e.g., Newell et al.[18] deduced a transfer time of approximately 1 yr in the upper troposphere). The global accumulation of NO_y had a time constant of approximately 1.5 yr, which corresponded to the time taken for NO_y to be transported from 20 to 8 km in this model. This time scale may be derived by comparing total accumulated mass of NO_y at equilibrium ($=3.76\times10^{34}$ molecules) with the source of 2.5×10^{34} molecules/year.

The computation was continued until the additional mass of NO_y at all locations resulting from the specified source was within 2% of the equilibrium value, a condition that was verified not only by studying the accumulation of NO_y with time but also by increasing NO_y by 2% at all grid points and noting the tendency for the total mass of NO_y to decrease with time. Equilibrium was attained after approximately 25 yr of integration: this integration time is characteristic of the transport parameters used in this model. It nevertheless illustrates that many years of integration with a two-dimensional model may be required in order to reach equilibrium (particularly in the hemisphere opposite to that of injection).

The calculated quasi-steady-state perturbations in NO_2 resulting from the midlatitude injection at 20 km (run 18) are shown in Fig. 3. These distributions were obtained at the time corresponding to the middle of the solsticial seasons in the two-dimensional model. The derived concentrations were equivalent to a 36% increase in total NO_y between 8 and 38 km. In the Northern Hemisphere, they consisted of an approximately 100% increase in NO_y below 20 km but decreased with altitude to an approximately 20% increase at 38 km. Throughout most of the Southern Hemisphere, the increase was 12–15%. The NO_2 increases were generally similar to those for NO_y except that, because the emission was initially in the form of NO_2, the delay in conversion to HNO_3 allowed NO_2 to attain an approximately tenfold increase at the injection location. Large percentage increases also are evident in winter at high latitudes of the Northern Hemisphere below 20 km alt.

The two-dimensional model yielded NO_2 concentrations up to 38 km alt. However, the three-dimensional model extended to 70 km, and some ozone destruction by NO_x occurred above 38 km. It therefore was assumed that the ratio of the NO_2 perturbations to the ambient NO_2 concentration was constant in each hemisphere above 38 km and was similar to the ratio calculated at 38 km. In the present calculation, a 20% increase thus was used in the Northern Hemisphere and a 10% increase in the Southern Hemisphere. The NO_2 perturbations above 38 km in Figs. 3-5 are based on an ambient NO_2 distribution obtained from Hesstvedt and Isaaksen[25] from a one-dimensional model. This ambient one-dimensional NO_2 distribution also was used to describe the NO_2 distribution above 38 km in the three-dimensional calculation of the unperturbed stratosphere.

A second perturbed stratosphere calculation was performed for a similar steady injection rate (1.8×10^6 tons/yr of NO_2)

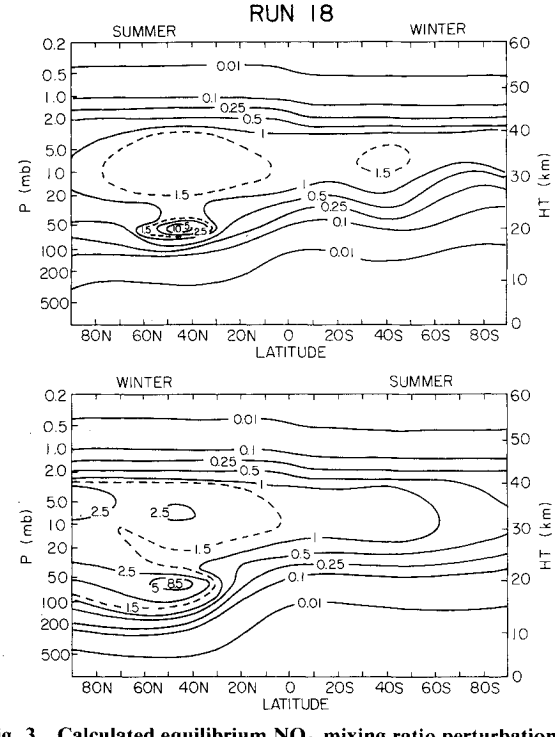

Fig. 3 Calculated equilibrium NO_2 mixing ratio perturbations for an injection of 1.8×10^6 tons/yr at 45°N, 20 km (run 18). The upper and lower parts of the figure represent summer and winter conditions, respectively, in the Northern Hemisphere. Units are parts per billion by volume.

initiated in year zero and inserted at 17 km alt again in the ratios 1:2:1 at 50°, 45°, and 40°N. The NO_2 distributions thus obtained are shown in Fig. 4 (run 19). The increase in total NO_y between 8 and 38 km relative to the unperturbed stratosphere was 27%. This increase consisted of an approximately 100% increase below 17 km but decreasing with increasing altitude to an approximately 12% increase at 38 km in the Northern Hemisphere. In the Southern Hemisphere, the increase was typically 12%. Above 38 km, a 12% increase was assumed in the Northern Hemisphere and a 10% increase in the Southern Hemisphere.

Transequatorial transport apparently occurred in the two-dimensional model throughout the 15–30-km-alt range but particularly in the middle stratosphere. The rather slow interhemispheric transport rate in this model may be producing unrealistically small Southern Hemisphere NO_2 concentrations in each of these calculations. However, an examination of our three-dimensional results indicates that the relative ozone depletions between hemispheres appear to be controlled more by the dynamics of the three-dimensional model (in which transequatorial transport rates are faster) than by the relative partitioning of NO_2 between hemispheres.

The third calculation assumed a tropical source, again of magnitude 1.8×10^6 tons/yr of NO_2, located at 20 km and in the ratios 1:2:1 at 15°, 10°, and 5°N. The equilibrium NO_2 distributions are shown in Fig. 5 (run 20). Since in this case the source was located in the rising branch of the Hadley circulation, this experiment produced the largest accumulation of NO_y between 8 and 38 km, with an increase of 55% over ambient concentrations. The magnitude of the tropospheric increase was similar to that of the two previous calculations but was divided more evenly between hemispheres (in the ratio approximately 2:1). Above 25 km, the increases in each hemisphere were similar and of magnitude approximately 33%. Above 38 km, a 33% increase in NO_2 was assumed in each hemisphere.

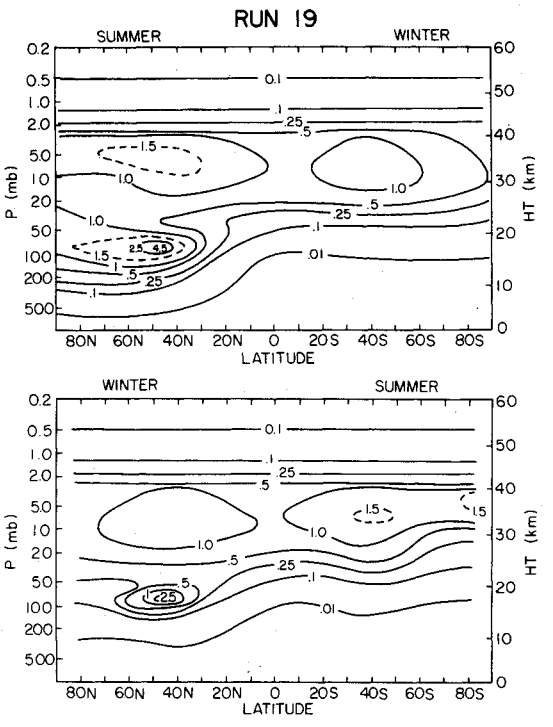

Fig. 4 Calculated equilibrium NO_2 mixing ratio perturbations for an injection of 1.8×10^6 tons/yr at 45°N, 17 km (run 19). The upper and lower parts of the figure represent summer and winter conditions, respectively, in the Northern Hemisphere. Units are parts per billion by volume.

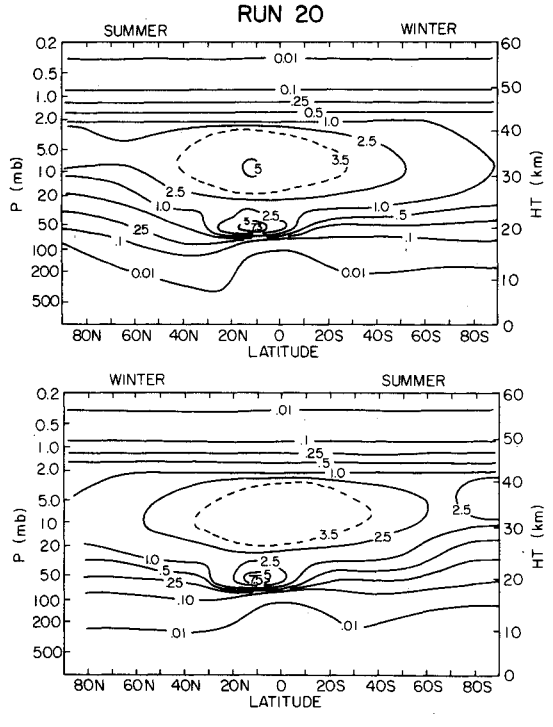

Fig. 5 Calculated equilibrium NO_2 mixing ratio perturbations for an injection of 1.8×10^6 tons/yr at 10°N, 20 km (run 20). The upper and lower parts of the figure represent summer and winter conditions, respectively, in the Northern Hemisphere. Units are parts per billion by volume.

Ozone Depletions

Ozone depletions have been calculated using a three-dimensional photochemical-dynamical model of the atmosphere.[6] This model possesses 36 levels at approximately 3-km intervals between the ground and 70 km alt and covers the entire globe. The horizontal resolution is approximately 2000 km at midlatitudes. Dynamical equations derived using the quasigeostrophic assumption are used to predict temperature, stream functions, and vertical velocity, as well as the distribution of atmospheric ozone. Transports of heat, momentum, and ozone are predicted explicitly. A small vertical diffusion term is included in this model to represent vertical transport by subgrid scale motions; the value of K_z used was an order of magnitude smaller than in Ref. 6 and was only 10^2 cm^2/sec at the tropopause. In this model, forcing of the motion field is produced by heating; solar heating due to ozone is recalculated at each time step as a function of the predicted ozone column, and infrared effects are treated by a Newtonian cooling approximation. Thus there exists strong coupling between ozone and the motion field. Integration proceeds using 1-hr steps throughout three annual cycles, with the solar declination angle changing continuously.

The chemistry of the three-dimensional model includes the Chapman reactions for odd oxygen, two reactions of odd hydrogen with atomic oxygen which affect ozone concentrations only above 50 km alt, and the following three reactions involving odd nitrogen

$$NO + O_3 \rightarrow NO_2 + O_2, \quad k = 1.7\times10^{-12}e^{-1310/T}\,cm^3 - sec^{-1}$$

$$NO_2 + O \rightarrow NO + O_2, \quad k = 9.1\times10^{-12}\,cm^3\text{-}sec^{-1}$$

$$NO_2 + h\nu \rightarrow NO + O, \quad \lambda < 3975\ \text{Å}$$

where T is the temperature. These three equations define the ratio of NO to NO_2 but require that the distributions of either NO_x or NO or NO_2 be prescribed. Ideally we should impose an NO_x distribution, since NO_x is better conserved than either

NO or NO_2; however, to reduce computation time NO_2 was prescribed based on the fact that NO_2 is the predominant form of NO_x in the altitude range in which most of the ozone destruction occurs (25–35 km).

The model neglects the destruction of O_3 by OH because the chemistry of the two-dimensional model produces hydroxyl concentrations which have only a small (~10%) effect on ozone. The principal effect of underestimating hydroxyl concentrations (see the discussion of the previous section) is that the relative importance of NO_x for ozone destruction may be overestimated.

A 3-yr integration of this model was performed first for the unperturbed stratosphere. It was noted that the dynamics settled down after only a few months integration but that it was not until the third year that ozone settled down into an annual cycle.

The NO_2 distribution used in the unperturbed stratosphere calculation (run 17) was based upon a two-dimensional calculation by Hesstvedt[19] and not our two-dimensional calculation for the unperturbed stratosphere. Figure 2 depicts that distribution during Northern Hemisphere summer conditions. During the Northern Hemisphere winter, a mirror image of that distribution was assumed. Between these seasonal extremes, a cosinusoidal variation with time was used. Above 35 km alt, a one-dimensional distribution of NO_2 calculated by Isaaksen and Hesstvedt[25] was used. We would, of course, have preferred to have used the NO_2 distribution shown in the upper portion of Fig. 2 for the unperturbed stratosphere. However, the necessity of obtaining rapid results for the Climatic Impact Assessment Program prevented us from awaiting the results of our two-dimensional model before commencing the three-dimensional unperturbed stratosphere calculation. The computation time of 12 hr for each 3-yr integration on the IBM 360/95 and the unlikelihood of significantly different results for either the perturbed or unperturbed stratosphere dissuaded us from rerunning the calculations at a later date. In particular, a comparison of the two portions of Fig. 2 suggests that the two unperturbed stratospheric distributions of NO_2 possess vertical structures that are similar relative to the range of possible structures that are consistent with current observations of NO_2.

The predicted zonal mean ozone distribution during Northern Hemisphere winter is shown in Fig. 6. The latitudinal variation of ozone is similar to that observed, but,

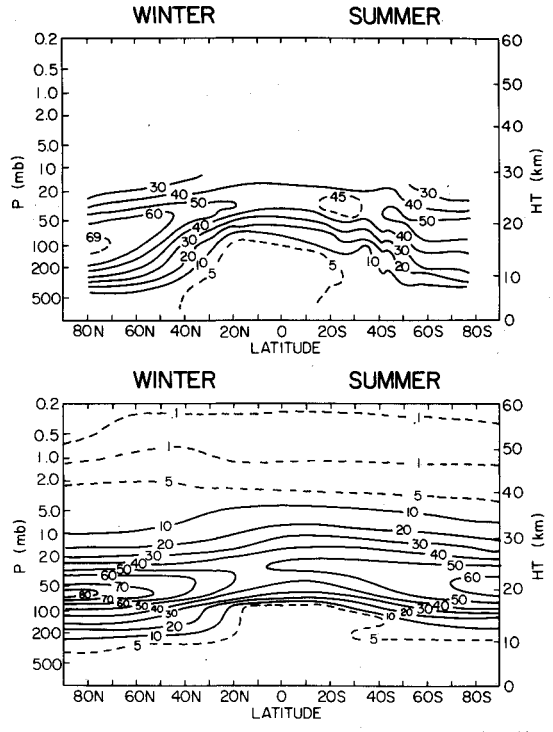

Fig. 6 Calculated and observed ozone concentrations (10^{11}/cm^2) for winter on the left and summer on the right. The upper drawing is based on values illustrated by Wu.[24] The lower part of the figure shows results for Northern Hemisphere winter in the third year of integration (season 12) of the three-dimensional calculation for the unperturbed stratosphere.

because transport through the tropopause is approximately 10 tons/sec (compared with approximately 25 tons/sec observed), ozone concentrations in the lower stratosphere are a little too high and concentrations in the troposphere are too low. Nevertheless, the simulated seasonal variation of ozone (which is included in Fig. 8) indicates that the calculated ozone distribution is remarkably similar to the observed variations of total ozone in the Northern Hemisphere (compare Fig. 3 of Ref. 4).

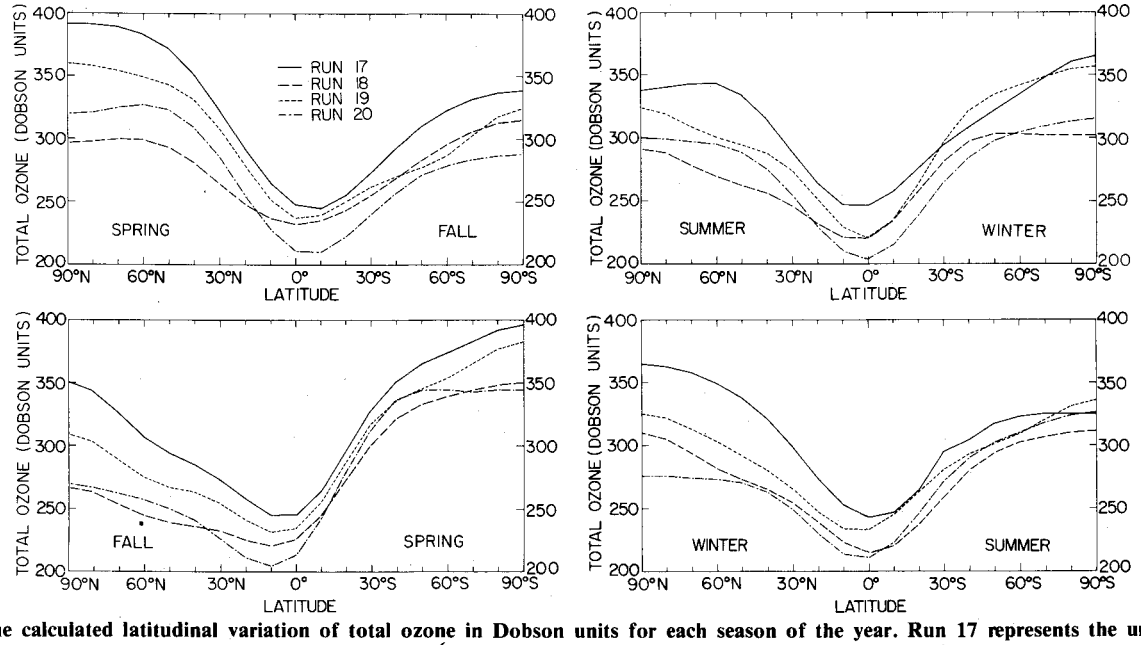

Fig. 7 The calculated latitudinal variation of total ozone in Dobson units for each season of the year. Run 17 represents the unperturbed stratosphere. Runs 18–20 represent the injection of 1.8×10^6 tons/yr of NO_2 at 45°N, 20 km; 45°N, 17 km; and 10°N, 20 km, respectively.

Following the unperturbed stratosphere calculations, three independent 3-yr integrations of the three-dimensional model were performed. The only difference between the parameters controlling each of these calculations was the different prescribed NO_2 distributions. These NO_2 distributions were derived in the similar manner from the two-dimensional model results. The Northern Hemisphere summer NO_2 perturbations shown in Figs. 3-5 were added individually to the NO_2 values shown in the lower portion of Fig. 2. The resulting distributions were assumed to represent Northern Hemisphere summer conditions in response to the continuous injection of NO_2 at various locations. Similarly, the NO_2 perturbations shown in the lower portions of Figs. 3-5 were added to the mirror image of the NO_2 distribution shown in the lower portion of Fig. 2 to represent Northern Hemisphere winter conditions. For application to the three-dimensional model, these six NO_2 distributions were assumed to be longitudinally invariant and to exist at the solstices in each of the three experiments. Between the solstices, cosinusoidal variations with 360-day (=1 model year) periods were assumed.

As an aid in the interpretation of our results, the calculated NO_2 and O_3 distributions have been averaged annually and also averaged over latitude and longitude (see Table 1). In all of the model runs, there was an excess production of ozone at approximately 25 km of order 10 tons/sec. This excess production was transported downward and, except for approximately 1 ton/sec, which was removed chemically between 15 and 20 km, was destroyed at the Earth's surface. In these calculations, eddy transports between 10 and 20 km were highly variable in both time and space. This variability below 20 km is responsible for the nonuniform ozone depletions at low altitudes shown in Table 1. This feature of the model is not expected to affect the overall model results, since 90% of the ozone is located above 17 km alt.

Each of the three calculations now will be discussed separately. Run 18 (source at 45°N and 20 km) yields a total ozone depletion that annually averages 11.9% and that is divided in the ratio approximately 2:1 between Northern and Southern Hemisphere (Table 2). There is no significant seasonal variation in this ratio. From Fig. 7, relative depletion maximizes between 45°N and the North Pole and is relatively uniform in the Southern Hemisphere in three of the four seasons. Moreover, the depletion at the latitude of injection (45°N) is not substantially larger than at other latitudes of the Northern Hemisphere. These effects also may be seen in Fig. 8, which shows similarly shaped contours in runs 17 and 18 and in which the most noticeable difference is at the North Pole in September, at which time the anomalous (i.e., not observed) maximum of run 17 is not found in run 18. From Table 1, we see that approximately 60% of the ozone depletion occurs below 22 km, with the greatest loss being produced at 20 km. Above 25 km, ozone is almost in chemical equilibrium, and the ozone depletions are related directly to the NO_2 distributions. Maximum sensitivity to NO_2 exists in the 35–40-km region, where the product of concentrations of NO_2 and atomic oxygen is maximum. Just above the ozone peak (e.g., ~25 km), the photodissociation coefficient of ozone has maximum sensitivity to the local ozone concentration, and thus an increase in NO_2 tends to be compensated by a reduction in the atomic oxygen concentration, so that the net loss of odd oxygen by the reaction between NO_2 and O changes little.

The relative depletion of ozone between hemispheres is dominated by ozone concentrations below 27 km, particularly between 18 and 26 km, a region in which transport effects play an important role. Between 23.5 and 26.1 km, the total mass of ozone is approximately 6×10^8 tons, and the production rate of odd oxygen is approximately 70 tons/sec; thus in this region ozone tends to be replenished chemically in roughly three months, and, since model transequatorial transport times were several years, the ratio of depletion in the Northern Hemisphere to that in the Southern Hemisphere depends primarily on the relative NO_x concentrations between hemispheres. At this level, a depletion ratio of approximately 2:1 was calculated. Between 18.3 and 20.9 km, the total mass of ozone is approximately 5×10^8 tons, and the production rate is approximately 6 tons/sec; thus at 20 km ozone tends to

Table 1 Globally averaged ozone concentrations ($\times10^{-10}$ cm^{-3}) and NO_2 volume mixing ratios ($\times10^8$)(in brackets) for each model calculation

Pressure, mb	Approximate altitude, km	Run 17	Run 18	Run 19	Run 20
2.28	41.9	42 [0.340]	38 [0.391]	40 [0.377]	38 [0.453]
3.43	38.8	64 [0.690]	56 [0.822]	58 [0.788]	49 [0.982]
5.15	35.9	108 [0.870]	96 [1.025]	100 [0.986]	85 [1.216]
7.71	33.0	163 [0.980]	149 [1.145]	154 [1.100]	135 [1.135]
11.6	30.2	251 [0.805]	234 [0.965]	240 [0.922]	214 [1.163]
17.3	27.5	389 [0.509]	366 [0.623]	373 [0.588]	336 [0.780]
26.0	24.8	508 [0.257]	488 [0.326]	491 [0.302]	465 [0.378]
39.0	22.2	529 [0.129]	482 [0.182]	496 [0.154]	482 [0.238]
58.5	19.6	478 [0.076]	306 [0.197]	389 [0.101]	395 [0]
87.8	17.1	217 [0.051]	200 [0.090)	170 (0.101]	229 [0.061]
132.0	14.6	64 [0.016]	70 [0.033]	108 [0.033]	50 [0.019]
198.0	12.0	50 [0.007]	28 [0.011]	50 [0.012]	30 [0.008]
296.0	9.3	22	20	30	18
444.0	6.4	25	19	27	19
667.0	3.4	27	22	32	22
1000.0	0.1	29	24	34	24

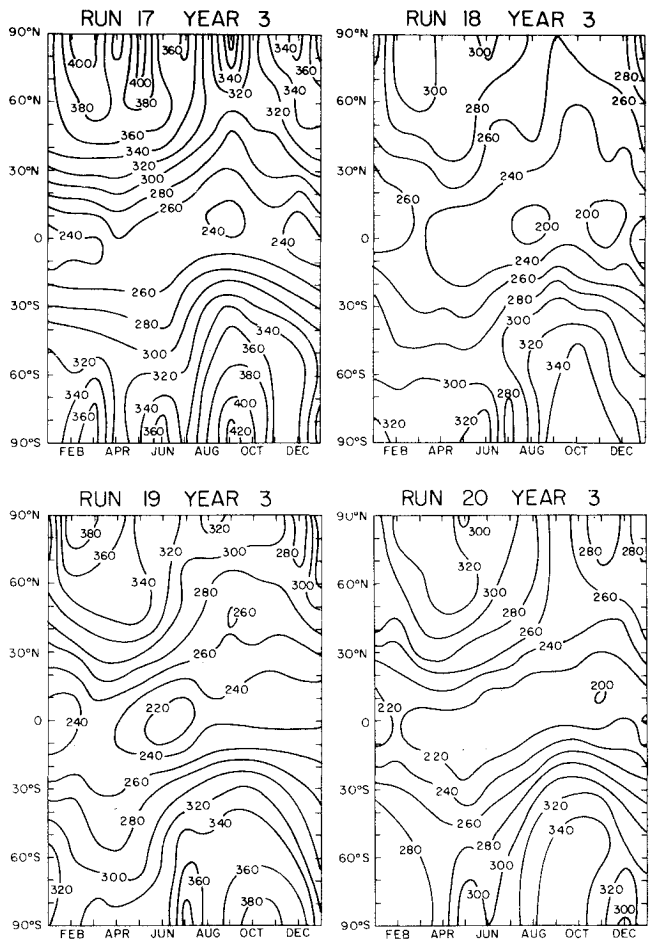

Fig. 8 The calculated latitudinal and seasonal variation of total ozone (Dobson units). The significance of the run numbers is the same as in Fig. 7.

be replenished chemically in 2 or 3 yr, a time longer than the 1-2-yr transequatorial transport time associated with a horizontal flux of order 10 tons/sec. At 20 km, therefore, any localized chemical loss tends to be smoothed horizontally. In particular, the additional loss of 3.5 tons/sec in run 18 at midlatitudes of the Northern Hemisphere (at 20 km) is balanced by eddy transport of ozone from the Southern Hemisphere (and by additional production of 1.5 tons/sec in the tropics as a result of increased penetration of ultraviolet radiation due to diminished ozone concentrations at higher altitudes). We calculated a Northern Hemisphere to Southern Hemisphere depletion ratio at 20 km equal to approximately 3:2. Integrating from 0-70 km gives a net interhemispheric depletion ratio in run 18 of approximately 2:1.

From Fig. 7, we note relatively uniform ozone depletion from 10°S to the South Pole but that depletion tends to increase with latitude from 10°S to the North Pole. This is the result of the maximum net loss of ozone occurring in the region of the maximum NO_x perturbation in the Northern Hemisphere and of the relatively uniform NO_x perturbation in the Southern Hemisphere. However, at high latitudes the concentrations are controlled primarily by ozone transports from middle lattitudes, and there is a tendency for the depletion at high latitudes of the Northern Hemisphere to exceed the loss at middle latitudes at that time of year (during winter and spring) when the high latitude concentrations have maximum sensitivity to the horizontal transport.

An analysis similar to that for run 18 can be applied to the run 19 results. However, because of the smaller ozone depletions in run 19, the calculations are influenced by differences in eddy transports between perturbed and unperturbed stratospheres.§ These differences are probably due to natural variability of our model atmosphere and not to real differences in correlations between ozone mixing ratios and velocities. The principal result of run 19, which is unlikely to be modified by small variations in eddy transports, is that the total ozone depletion in run 19 was approximately 6% or one-half of that for a source at 3 km higher altitude. This depletion is shown in Table 1, in which we see that the depletion above 22 km for runs 18 and 19 is in the ratio 3:2, which corresponds to the ratio of NO_2 perturbations at those altitudes. However, at 20 km the ozone depletion is substantially less in run 19 than in run 18 because the maximum NO_2 perturbation occurred at 17 km in run 19. The much larger ozone depletion below 22 km in run 18 is responsible for the 2:1 depletion ratio between runs 18 and 19.

The run 20 results do not suffer generally from the limitations encountered in run 19. The total ozone depletion in run 20 was 12.5%. This is remarkably similar to that

§Run 19 results indicate that the total ozone below level 18 was greater in the perturbed stratosphere (see Table 1), that the ozone in middle latitudes of the Southern Hemisphere during winter increased in run 19 (this is seen as a small phase shift of the total ozone in Fig. 8), and that the Northern Hemisphere to Southern Hemisphere depletion ratio averaged 2:1. The last result is questionable because the more uniform horizontal distribution of NO_2 in the stratosphere in run 19 than in run 18 and the substantially diminished ozone depletion at approximately 20 km (see Table 1) would be expected to produce a smaller interhemispheric depletion ratio than in run 18.

Table 2 The ratio of hemispheric ozone concentrations for the perturbed stratosphere and the unperturbed stratosphere for each season of the third year of integration (expressed as percentages)

		March-May	June-Aug.	Sept.-Nov.	Dec.-Feb.	Annual mean
(Run 18/run 17) ×100%	Northern hemisphere	82.6	84.1	84.5	84.3	83.9
	Southern hemisphere	93.5	92.8	91.6	91.3	92.3
	Global mean	87.7	88.5	88.3	87.8	88.1
(Run 19/run17) ×100%	Northern hemisphere	94.0	91.6	92.3	89.1	91.8
	Southern hemisphere	94.1	98.7	96.0	97.5	96.6
	Global mean	94.0	95.1	94.3	93.2	94.2
(Run 20/run 17) ×100%	Northern hemisphere	86.3	86.4	83.2	81.7	84.5
	Southern hemisphere	86.7	89.0	92.8	93.8	90.6
	Global mean	86.5	87.7	88.3	87.6	87.5

obtained in run 18, despite substantial differences between the NO_2 distributions in the two calculations and between the altitude distributions of the ozone depletions. In run 20 there was more NO_2 in the middle and upper stratosphere than in the previous calculations because NO_2 was being injected where the motion of the atmosphere is predominantly upward. The increased NO_2 concentrations above 20 km produced more ozone depletion there but were counterbalanced by the small atomic oxygen concentrations in the tropics at 20 km, thus resulting in substantially less ozone loss at that level than in run 18 (see Table 1). Below 25 km the NO_2 perturbation was hemispherically asymmetric (Fig. 5), and there was sufficient ozone depletion in run 20 below 25 km to produce some asymmetry of depletion between the hemispheres. In Table 2, we report approximately 5:3 for the ratio of the depletion of the Northern Hemisphere to that of the Southern Hemisphere. This ratio is, however, seen to vary seasonally, with largest depletions occurring in fall and winter. This result is produced by the horizontal motions: maximum depletion in the Southern Hemisphere occurs when that hemisphere is most dependent on Northern Hemisphere production, that is, during Southern Hemisphere winter, at which time ozone is being transported from the Northern Hemisphere into the Southern Hemisphere. In contrast, depletion is least when most of the hemisphere is dependent only weakly on tropical production, that is, during summer, when motions are weak and midlatitude concentrations are controlled by decay from the spring accumulation. The depletion maximum in the fall is associated primarily with additional eddy transport from the fall to the spring hemisphere at the tropopause. There is no obvious reason for this change in eddy flux of ozone between runs 17 and 20, and we regard the calculated spring/fall hemispheric depletion ratio as requiring additional substantiation, which might be obtained by one or two more years of model integration.

The latitudinal variation in ozone for run 20 is shown in Fig. 7. Because proportionally more depletion occurs at higher altitudes where ozone is in photochemical equilibrium, the depletion possesses a more pronounced maximum at the latitudes of injection than in runs 18 and 19. Apart from this effect, the depletions are fairly uniform in latitude except for a tendency for larger depletions in the polar region occurring, as in run 18, because of a filtering action on the poleward ozone fluxes.

Discussion

Our calculations utilized an NO_2 emission rate of 1.8×10^6 tons/yr. Based on current emission levels,[20] this emission rate would be provided by ~2000 Concordes operating 8 hr/day (which cruise at approximately 17 km alt). However, not only are the emission levels of future fleets of SST's uncertain, but significant uncertainties remain in the chemistry of the atmosphere. Therefore, large error bars must be assigned to the calculations of this paper in estimating the absolute magnitude of the future ozone depletion due to SST's.

The calculation procedure employed clearly was not optimum because of the weak coupling that existed between the two- and three-dimensional models. The residence time of material in the lower stratosphere was approximately 2 yr in the two-dimensional model, in agreement with observation. We thus would expect that approximately the "correct" amount of NO_y is being retained in the model stratosphere. The interhemispheric transport time in the two-dimensional model was significantly longer than that in the three-dimensional model (which was in better agreement with observation). It is likely, therefore, that NO_2 concentrations in the Southern Hemisphere have been underestimated and thus that the interhemispheric ozone depletion ratio has been overestimated. Moreover, although we would have expected a smaller depletion ratio in the case of a tropical injection than for a midlatitude injection, there was sufficient variability of the horizontal eddy fluxes responsible for this ratio near the tropopause so that we limit our conclusion as follows: each of our calculations resulted in at least half as much ozone depletion in the Southern Hemisphere as in the Northern Hemisphere.

The weak coupling between the two- and three-dimensional models also had the consequence that chemical feedbacks involving NO_x and ozone were neglected. Some assessment of the importance of the chemical feedbacks was obtained in an experiment with the two-dimensional model, in which the prescribed ozone concentrations were reduced arbitrarily by 10%.[7] It was concluded that the influence of ozone changes on the natural cycle for NO_x production from N_2O was small. The effect of decreased ozone concentrations on the partitioning of NO_y between NO, NO_2, and HNO_3 also was considered, and it was concluded that NO_2 concentrations could increase significantly at 20 km alt. Despite this last conclusion, we did not feel that the magnitude of the effect was sufficient to justify additional calculations of this particular problem using the current modeling procedure.

As pointed out in a previous section, recent evidence suggests that calculated hydroxyl concentrations are unrealistically low. The principal effect of this discrepancy would be to overestimate the importance of nitrogen oxides in the global ozone balance. Furthermore, the uncertainty in estimated potential ozone destruction is compounded by the possibility that other anthropogenically produced chemicals capable of affecting the ozone balance will continue to be added to the atmosphere. In particular, fluorocarbons not only are likely to have some effect on ozone[21] but also may affect the NO_x balance through the formation of chlorine nitrate.[22] Based upon these various uncertainties, we conclude that relative ozone depletions presented in this paper are more meaningful than absolute magnitudes of those depletions.

Conclusions

Calculations have been reported of the atmospheric ozone depletions produced by injections of NO_2 at two latitudes and two altitudes in the Northern Hemisphere. We found that injections at 45°N and 10°N (at 20 km alt) resulted in similar global ozone depletions, and we thus conclude that the global depletion of ozone resulting from supersonic flight is relatively independent of the latitude of the flight corridor. The calculations also showed, however, that more nitrogen oxides were retained in the stratosphere in the case of a tropical injection than for a midlatitude injection; this effect was offset by the smaller atomic oxygen concentrations existing in the tropical lower stratosphere which resulted in less ozone depletion for a specified concentration of NO_2. This result points out that it is not possible to relate ozone depletion directly to the NO_x increase, as often is done in one-dimensional models.

A comparison of the results for 17 and 20 km alt at midlatitudes showed twice as much ozone depletion globally for the higher injection altitude. This result illustrates the sensitivity of ozone depletion to the altitude of supersonic flight.

The global nature of the ozone depletion was indicated by the result that, although the nitrogen oxide injections occurred in the Northern Hemisphere, a considerable ozone depletion was calculated in the Southern Hemisphere. In fact, in all calculations at least half as much ozone depletion occurred in the Southern Hemisphere as in the Northern Hemisphere. Only in the case of the tropical injection was a seasonal variation of this hemispheric depletion ratio noted, with larger ozone depletions occurring in the Southern Hemisphere in winter than in summer.

All of these calculations were performed using a two-dimensional model of the atmosphere to calculate the resulting ozone depletion. Improvements in this procedure are envisaged in the future by using a larger and faster machine, which should permit nitrogen oxides and ozone to be calculated simultaneously in the three-dimensional model. At

that time, the chemistry of odd hydrogen in the model will be updated to reflect the increased importance now expected for odd hydrogen in the atmospheric ozone balance. We do not expect, however, that these model improvements will produce the significant changes in the conclusions on relative ozone depletions stated in the foregoing.

Acknowledgments

This research was supported by the Atomic Energy Commission and the Department of Transportation under Contract AT(11-1)-2249 and by NASA under Grants NSG-2010 and NGR-22-009-729 (computer time).

References

[1] "Environmental Impact of Stratospheric Flight," National Academy of Sciences, Washington, D.C., 1975.

[2] Grobecker, A. J., Coroniti, S. C., and Cannon, R. H., Jr., "The Effects of Stratospheric Pollution by Aircraft," Report of Findings, Dept. of Transportation, Washington, D. C., DOT-TST-75-50, Dec. 1974.

[3] "Committee on Meteorological Effects of Stratospheric Aircraft (COMESA), Final Report, 1972–1975," Dept. of Industry, London, England, 1975.

[4] Alyea F. N., Cunnold, D. M., and Prinn, R. G., "Stratospheric Ozone Destruction by SST-Induced NO_x," *Science,* Vol. 188, April 1975, p. 117.

[5] Widhopf, G. F., "Meridional Distributions of Trace Species in the Stratosphere and the Effect of SST Pollutants," *A. G. U. Fall Annual Meeting,* Dec. 1974, San Francisco, Calif.

[6] Cunnold, D. M., Alyea, F. N., Phillips, N. A., and Prinn, R. G., "A Three-Dimensional Dynamical-Chemical Model of Atmospheric Ozone," *Journal of Atmospheric Science,* Vol. 32, Jan. 1975, p. 170.

[7] Cunnold, D. M., Alyea, F. N., Phillips, N. A., and Prinn, R. G., "First Results of a General Circulation Model Applied to the SST-NO_x Problem," *Proceedings of the 2nd International Conference on the Environmental Impact of Aerospace Operations in the High Atmosphere,* July 8–10, 1974, American Meteorological Society, Boston, Mass., p. 187.

[8] Prinn, R., Alyea, F., Cunnold, D., and Katz, A., "The Distribution of Odd Nitrogen and Odd Hydrogen in the Natural and Perturbed Stratosphere," *Proceedings of the 2nd International Conference on the Environmental Impact of Aerospace Operations in the High Atmosphere,* July 8–10, 1974, American Meteorological Society, Boston, Mass., p. 179.

[9] Prinn, R. G., Alyea, F. N., and Cunnold, D. M., "Stratospheric Distribution of Odd Nitrogen and Odd Hydrogen in a Two-Dimensional Model," *Journal of Geophysical Research,* Vol. 80, Dec. 1975, p. 4997.

[10] Hering, W., 'Ozone and Atmospheric Transport Processes," *Tellus,* Vol. 18, 1966, p. 336.

[11] Hering, W. and Borden, T. R., Jr., "Ozonesonde Observations over North America," Vol. 2, Air Force Cambridge Research Labs., Cambridge, Mass., Environmental Research Papers 38, AFCRL-64-30 (II), 1964.

[12] Hering, W. and Borden, T.R., Jr., "Ozonesonde Observations over North America," Vol. 3, Air Force Cambridge Research Labs., Cambridge, Mass., Environmental Research Papers 279, AFCRL-64-30 (IV), 1967.

[13] Hering, W. and Borden, T. R., Jr., "Ozonesonde Observations over North America," Vol. 4, Air Force Cambridge Research Labs., Cambridge, Mass., Environmental Research Papers 279, AFCRL-64-30 (IV), 1967.

[14] Gudiksen, P., Fairhall, A., and Reed, R., "Roles of Mean Meridional Circulation and Eddy Diffusion in the Transport of Trace Substances in the Lower Stratosphere," *Journal of Geophysical Research,* Vol. 73, July 1968, p. 4461.

[15] Ackerman, M., "NO, NO_2 and HNO_3 Below 35 km in the Atmosphere," *Aeronomica Acta,* Vol. 142, 1975.

[16] Noxon, J. F., "Nitrogen Dioxide in the Stratosphere and Troposphere Measured by Ground-Based Absorption Spectroscopy," *Science,* Vol. 189, Aug. 1975, p. 547.

[17] Anderson, J. G., "The Absolute Concentration of OH ($X^2\pi$) in the Earth's Stratosphere," *Geophysical Research Letters,* Vol. 3, March 1976, p. 165.

[18] Newell, R. E., Vincent, D. G., and Kidson, J. W., "Interhemispheric Mass Exchange from Meteorological and Trace Substance Observations," *Tellus,* Vol. 21, 1969, p. 641.

[19] Hesstvedt, E., "A Simplified Time-Dependent Two-Dimensional Photochemical Model of the Stratosphere," *Proceedings of the IAMAP First Special Assembly,* Jan. 14–25, 1974, Melbourne, Australia.

[20] "Propulsion Effluents in the Stratosphere," Dept. of Transportation, Washington, D. C., CIAP Monograph 2, Sept. 1975.

[21] "National Academy of Sciences, Halocarbons: Effects on Stratospheric Ozone," Report of the Panel on Atmospheric Chemistry, National Academy of Sciences, Washington, D. C., Sept. 1976.

[22] Rowland, R. S., Spencer, J. E., and Molina, M. J., "The Stratospheric Chemistry of Chlorine Nitrate, $ClONO_2$," Dept. of Chemistry, Univ. of California, Irvine, Calif. 1976.

[23] Lazrus, A. L. and Gandrud, B., "Distribution of Stratospheric Nitric Acid Vapor," *Journal of Atmospheric Science,* Vol. 31, May 1974, p. 1102.

[24] Wu, M. F., "Observations and Analysis of Trace Constituents in the Stratosphere," Environmental Research Technology, Lexington, Mass., Annual Rept., Contract DOT-05-20217, July 1973.

[25] Hesstvedt, E. and Isaaksen, I., private communication, 1974.